Direct observation of Bose-Einstein condensation in a parametrically driven gas of magnons.

O Dzyapko[1], V E Demidov[1], S O Demokritov[1], G A Melkov[2] and A N Slavin[3]

[1]Institute for Applied Physics, University of Münster, Germany

[2]Department of Radiophysics, National Taras Schevchenko University of Kiev, Kiev, Ukraine

[3]Department of Physics, Oakland University, Rochester, MI, USA

Abstract. A gas of thermalized quasi-equilibrium magnons with a non-zero chemical potential created in a magnetic film using parametric pumping is studied. The value of the chemical potential of the gas is determined directly from the measured distribution of magnons over the spectrum. With increasing pumping power the value of the chemical potential increases. At high enough pumping powers it reaches the energy corresponding to the lowest magnon frequency. Under these conditions a very narrow peak of magnon population at the lowest magnon frequency appears. The measured width of the peak is five orders of magnitude smaller than that expected for the thermal distribution. We associate this effect with Bose-Einstein condensation of magnons.

Bose-Einstein condensation (BEC) is one of the most striking manifestations of quantum nature of matter on the macroscopic scale. It represents a formation of a collective quantum state of particles with integer spin – bosons. In 1925 Einstein, using the method proposed by Bose, has shown that in a gas of bosons the density of particles with energy ε is described by the occupation function:

$$n(\varepsilon) = (\exp((\varepsilon - \mu)/k_B T) - 1)^{-1}, \quad (1)$$

where ε is the energy of the particle, T is the temperature, and k_B is the Boltzman constant [1]. The chemical potential μ is determined from the condition for the total density of the particles, N:

$$N = \int_{\varepsilon_{\min}}^{\infty} D(\varepsilon) n(\varepsilon) d\varepsilon \ , \quad (2)$$

where $D(\varepsilon)$ is the density of states of the particles. As the density of the particles, N, increases at a given temperature T, the chemical potential μ increases as well. On the other hand, it is seen from Eq. (1) that μ cannot be larger than the minimum energy of the particles $\varepsilon_{min.}$ Thus, Eq. (2) with $\mu = \varepsilon_{min}$ defines a critical density $N_c(T)$. If the density of the particles in the system is larger than N_c, BEC takes place: the gas is spontaneously divided into two fractions: particles with the density N_c distributed according to Eq. (1) with $\mu = \varepsilon_{min}$ and particles accumulated in the ground state with $\varepsilon = \varepsilon_{min}$. The latter fraction represents a Bose-Einstein condensate [1].

During the last decades many efforts have been made to observe the BEC transition in a gas of atoms. Estimations show that in this case an extremely low temperature is needed to decrease the critical density N_c to experimentally achievable densities of the atomic gas. Using a laser cooling technique and an enforced evaporation of atoms from a trap atomic BEC was observed in diluted atomic gases at temperatures of 10^{-7} K [2,3]. Somewhat less extreme experimental conditions are needed to achieve BEC in a gas of quasi-particles in solids, which makes quasi-particle gases to be a convenient model system for studying this phenomenon. A gas of quasi-particles is a very attractive object for the observation of BEC for the following reasons: (i) since the effective mass of quasi-particles can be essentially smaller than that of atoms, the BEC transition should occur at higher temperatures; (ii) a large number of quasi-particles exists at non-zero temperatures due to thermal fluctuations; (iii) if necessary, the density of quasi-particles can be increased using different methods of external excitation such as microwave pumping [4] or illumination with laser light [5]. At the same time a possibility of BEC in quasi-particle gases is not evident from the point of view of thermodynamics, since quasi-particles are characterized by a finite lifetime, which is often comparable to the time needed to reach thermodynamic equilibrium [6]. Therefore, BEC in a gas of quasi-particles can be only realized, if the mean lifetime of the considered particles is much longer than their thermalization time defined by the scattering processes between the particles [7].

To date the observation of BEC of quasi-particles has been reported for excitons and biexcitons [5,8,9,10], polaritons [11,12], phonons [13], and magnons [14-18]. Note, that in all the above studies BEC was observed at cryogenic temperatures.

Magnons are quanta of excitations in the spin system of magnetically ordered crystals. At temperatures far below the temperature of magnetic ordering, T_c, magnons can be considered as weakly interacting bosons. Several groups have reported observation of the field induced BEC of magnons in quantum antiferromagnets $TlCuCl_3$ [14,15], Cs_2CuCl_4 [16,17], and $BaCuSi_2O_6$ [18]. In these materials a phase transition accompanied by a magnon mode softening occurs if the applied magnetic field is strong enough to overcome the antiferromagnetic exchange coupling. Such transition can be treated as BEC in a diluted

magnon gas. In order to achieve it relatively high magnetic fields, $H \sim 10^5$ Oe, and low temperatures, $T \leq 1$ K, are required. Very recently it has been shown [19] that BEC in a parametrically driven gas of magnons can be achieved at moderate magnetic fields and room temperature. The key feature of the latter observation is the use of low-loss dielectric ferrite films as a magnetic medium. These films are characterized by the very long magnon lifetime and intense magnon-magnon scattering. In this paper we present a detailed account of the experiments [19].

The experiments on room-temperature BEC of magnons were performed on thin monocrystalline films of yttrium iron garnet (YIG). YIG ($Y_3Fe_2(FeO_4)_3$) is a cubic ferrimagnetic insulator [20]. For relatively weak magnetic fields ($H < 10^5$ Oe) and for frequencies below 1 THz it can be considered as a ferromagnet due to the strong magnetic coupling between its sublattices. Due to its unique properties YIG is very well suited for experiments on Bose-Einstein condensation of magnons. First, there is an efficient way to control the density of the magnon gas in YIG films. It can be done by the energy transfer from microwave electromagnetic field to the magnon gas using parametric pumping [21]. This approach allows one to increase the entire density of magnons by 10^{18}-10^{19} cm^{-3}. Second, the mean lifetime of magnons τ_{sl} in high-quality YIG films exceeds 1000 ns due to the very weak spin-lattice relaxation [21]. This spin-lattice relaxation time is much longer than the characteristic time of magnon-magnon interaction, which for high density of magnons can be as small as $\tau_{ss} < 100$ ns [21]. Thus, thermalization of parametrically injected magnons can be achieved in the magnon gas, which is practically decoupled from the crystalline lattice. Under such circumstances a quasi-equilibrium magnon gas can be characterized by its own temperature and the chemical potential, which can deviate from those of the lattice. The third important advantage of YIG films as a medium for observation of BEC of magnons is their transparency for visible light. This allows one to apply a very sensitive and well-developed Brilloun light scattering (BLS) spectroscopy [22] for measurements of magnon distributions over frequencies/energies, which provide a direct way to address statistics of magnons.

Figure 1 shows the low-frequency part of the magnon spectrum in a ferromagnetic film magnetized by an in-plane static magnetic field. The spectrum of magnons is mainly determined by two interactions: the exchange interaction and the magnetic dipole-dipole interaction. The exchange interaction dominates for magnons with large wavevectors and leads to the quadratic dependence of frequency of magnons on their wavevector ($\omega \sim k^2$), which is reminiscent to the spectrum of free massive particles ($\varepsilon = (2m)^{-1}p^2$). In contrast, the long-range dipole-dipole interaction dominates in the region of relatively small wavevectors. Since this interaction is anisotropic, the spectrum of magnons in this wavevector interval is anisotropic as well, i.e., it depends on the angle between the vector of the static magnetic field, $\mathbf{H}_0$, and the magnon wavevector, $\mathbf{k}$. The purely dipolar (when the exchange interaction

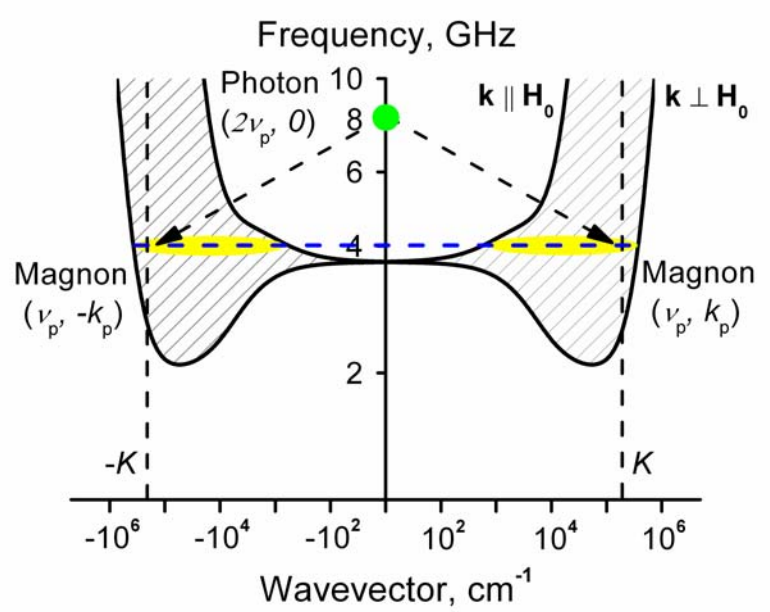

Figure 1. Energy spectrum of magnons in a thin ferromagnetic films magnetized by an in-plane static magnetic field. The low frequency part of the magnon spectrum is shown in the log-log-scale. The wavevector intervals of parametrically injected magnons are indicated in yellow. The wavevectror interval accessible for BLS measurements is limited by $\pm K$.

is neglected) spectrum of magnons in ferromagnetic films was calculated in [23]. In accordance with this work the lowest-frequency dispersion curve of magnons corresponds to the case $\mathbf{k} \parallel \mathbf{H}_0$. The frequency of these magnons monotonically decreases with increasing wavevector and approaches the frequency of the uniform ferromagnetic resonance in bulk ferromagnets. If both the exchange and the dipole-dipole interactions are taken into account [24], the lowest-frequency dispersion curve of magnons with $\mathbf{k} \parallel \mathbf{H}_0$ demonstrates a minimum at $k_{min} \neq 0$. This minimum corresponding to the absolute minimum of magnon frequency is clearly seen in figure 1. For 5 μm thick YIG films used in the experiment and a typical value of the applied magnetic field of $H_0 = 700$ Oe the minimum magnon frequency is $\nu_{min} = 2.09$ GHz. It corresponds to the wavevector $k_{min} \approx 5.5 \cdot 10^4$ cm^{-1}.

Figure 1 also illustrates the process of parametric pumping of the magnon gas. To realize this pumping one has to apply a dynamic microwave magnetic field oriented parallel to the direction of the applied static magnetic field $\mathbf{H}_0$. The spatially uniform pumping microwave field produces a modulation of the longitudinal component of the sample magnetization with the pumping frequency $2\nu_p$. This modulation causes a parametric excitation of two spin waves with the frequency ν_p and equal and oppositely directed wavevectors $\pm k_p$. This process can also be considered as a creation of two magnons by a photon of the pumping field. In this process the wavevectors of the created magnons, $\pm k_p$, and their frequencies, ν_p, are determined by the momentum and the energy conservation laws. In our experiments primary non-

equilibrium magnons were injected by parametric pumping at a frequency far from the frequency of the bottom of the magnon spectrum. Note here, that although the primary magnons are excited by a coherent pumping, they are not coherent to each other: two magnons are excited simultaneously, and only the sum of their phases, but not the phase of each magnon, is locked to the phase of the pumping. Moreover, at higher pumping powers the frequency of each magnon can slightly deviate from ν_p keeping, of course, the sum of two frequencies equal to the pumping frequency, $2\nu_p$ [21]. Due to the intense magnon-magnon interaction process the injected magnons were redistributed over the entire spectrum through multiple magnon-magnon scattering events and a new quasi-equilibrium state of the gas was formed.

From the point of view of thermodynamics the Bose-Einstein condensation can take place if the chemical potential reaches the value of the minimum energy in the magnon spectrum. As described above, the minimum frequency/energy of magnons in a ferromagnetic film is non-zero if an external static magnetic field is applied. On the other hand, at the thermal equilibrium the interaction between the magnon system and the lattice occurs through an exchange of particles (creation of magnons by phonons and vise versa). Since the number of magnons is not constant, but is determined by the thermodynamic laws, the chemical potential of magnon gas at the thermal equilibrium with the lattice is equal to zero ($\mu = 0$) [25]. In order to create a quasi-equilibrium magnon gas with a non-zero chemical potential ($\mu > 0$) one has to increase the number of magnons above the thermodynamic equilibrium level, which can be realized, for example, by applying an external energy flow. Besides, a conservation of the number of magnons in the magnon-magnon scattering processes should be guaranteed. Otherwise, the energy fed into the system will lead to an increase of the temperature of the gas keeping the chemical potential $\mu = 0$.

As was mentioned above, the characteristic time of the spin-lattice relaxation processes in YIG films significantly exceeds the magnon thermalization time determined by the nonlinear magnon-magnon interaction. This fact allows one to consider the spin-lattice relaxation as a small perturbation on the temporal scale much smaller than τ_{sl}. The four-magnon scattering (two magnons “in”, two magnons “out”) caused by the exchange interaction is the main mechanism for the magnon thermalization. This process obviously conserves the number of magnons. The same is valid for the elastic two-magnon process due to the scattering of magnons on impurities and surfaces of the film. On the contrary, three-magnon processes caused by the dipole-dipole interaction do not conserve the number of magnons, preventing the formation of BEC, if dominate. However, choosing an appropriate value of the applied static magnetic field, H_0, one can make these processes to be prohibited for the low-energy magnons important for observation of BEC by the energy and momentum conservation laws [21].

Another important restriction on the experimental conditions is that the so-called kinetic instability should be prohibited. This instability has been investigated in detail in [26]. It arises due to the compensation of the spin-wave damping by parametric pumping and might cause a strongly non-equilibrium distribution of magnons with a maximum near the point where the magnon dissipation has its minimum value. This effect, however, can be also avoided by an appropriate choice of the static magnetic field, H_0.

For the pumping frequency of $2\nu_p$=8.10 GHz used in our experiments the three-magnon processes are allowed for magnetic fields smaller than 650 Oe, whereas the kinetic instability appears for the fields larger than 1100 Oe. Consequently, the range of H_0=650-1100 Oe is appropriate for experimental observation of BEC. The absence of the above undesirable processes under the used experimental conditions was experimentally proved by observing the dynamics of redistribution of magnons over the spectrum after the start of the pumping pulse. This redistribution was found to be in a form of a gradual population of magnon states starting from the frequency of injected magnons towards the bottom of the spectrum, which is expected for thermalization of the magnon gas to a quasi-equilibrium state through the four-magnon scattering. The corresponding thermalization times have been found to be below 100 ns at the pumping powers important for the observation of BEC [27]. Therefore, time-resolved measurements reported here have been performed at delay times above 100 ns, to ensure that a quasi-equilibrium magnon gas was studied. Very similar results have been obtained for all values of the applied field between 650 Oe and 1100 Oe. In this paper we present the data obtained for the static magnetic field of H_0=700 Oe, which is shifted towards the lower limit of the allowed field range. This choice is explained by the fact that for smaller fields one can better resolve details of magnon distribution over frequencies.

Taking the chosen values of experimental parameters one can easily estimate the increase in the magnon density necessary for the chemical potential to reach the minimum magnon energy. As already mentioned, at the thermal equilibrium with the lattice the magnon gas has the chemical potential $\mu_0 = 0$. The density of magnons, N_0, and their energy density, E_0, are given by:

$$N_0 = \int_{\nu_{min}}^{\infty} D(\nu) n(\nu, \mu_0, T_0) d\nu$$

$$E_0 = \int_{\nu_{min}}^{\infty} h\nu D(\nu) n(\nu, \mu_0, T_0) d\nu$$

where T_0 is the temperature of the system (room temperature in our case). As explained above, parametric pumping creates additional δN magnons with the energy $\varepsilon_p = h\nu_p$, which are then redistributed over the spectrum mainly due to the fast nonlinear four-magnon interaction. A quasi-equilibrium state with chemical potential μ and temperature T is settled. For this state one can write

$$N = \int_{\nu_{\min}}^{\infty} D(\nu) n(\nu, \mu, T) d\nu$$

$$E = \int_{\nu_{\min}}^{\infty} h\nu D(\nu) n(\nu, \mu, T) d\nu$$

Since the four-magnon processes conserve the number of magnons and the energy relaxation into the lattice can be considered to be negligible, one should require $N = N_0 + \delta N$ and $E = E_0 + \delta E = E_0 + h\nu_p \delta N$. Using these relations it is possible to determine μ and T as a function of δN. Since the value of $\varepsilon_{\min} = h\nu_{\min}$ is rather small ($\varepsilon_{\min} << kT_0$) one can provide an increase of μ from zero to $\varepsilon_{\min}$ even for $\delta N << N_0$. Simple calculations based on the above equations show that for the used experimental conditions ($\nu_{\min} \approx 2$ GHz, $\nu_p \approx 4$ GHz) the necessary increase of the chemical potential can be achieved for densities of the injected magnons $\delta N \sim 5 \cdot 10^{18}$ cm^{-3}, which can be easily realized in experiments.

The setup for magnon excitation and observation of the BEC-transition is schematically shown in figure 2. Optically transparent single-crystalline YIG film with the crystallographic orientation (111) and the thickness of 5 μm was used in the experiment. The film was epitaxially grown on a gadolinium-gallium-garnet substrate with lateral dimensions of 2 × 20 mm^2. The film sample was mounted onto a microstrip resonator with resonant frequency of 8.10 GHz providing an intense electromagnetic pumping field. The system was placed into a spatially uniform static magnetic field $H_0 = 700$ Oe oriented in the film plane. The direction of the microwave electromagnetic field of the pumping resonator coincided with the direction of $\mathbf{H}_0$, i.e., the geometry of the parallel parametric pumping was realized. To avoid an

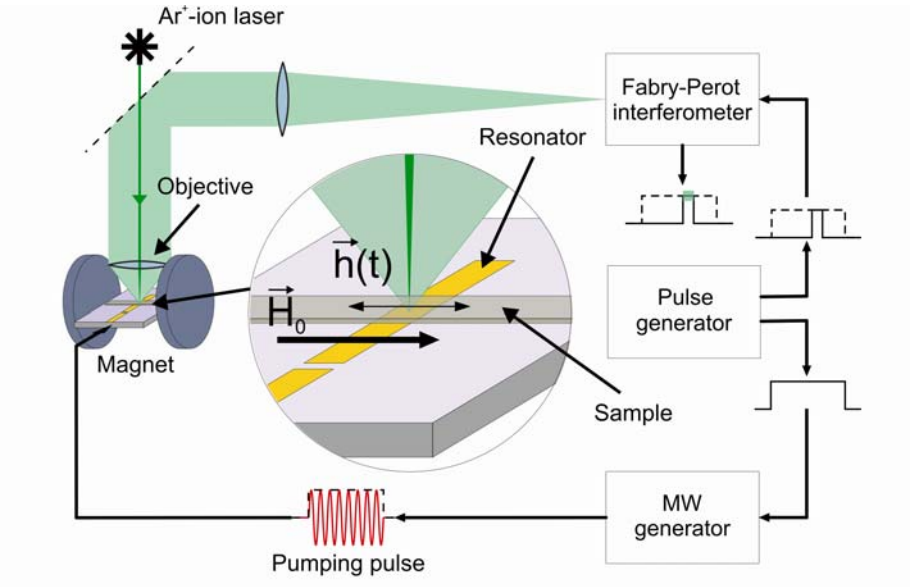

Figure 2. The experimental setup for time-resolved BLS measurements of distribution of magnons over frequencies in a parametrically driven magnon gas.

overheating of the YIG sample by microwaves the pumping was performed in the pulsed regime. The duration of pumping pulses was $\tau_p = 1$ μs, which was sufficient to guarantee that the quasi-equilibrium state of the driven magnon gas is established and to allow the investigation of the evolution of the magnon gas during the pulse. The repetition period of $t_p = 20$ μs was chosen to be large enough in order the magnon gas to return to its initial thermal state between pulses.

As discussed above, the application of parametric pumping leads to an excitation of primary magnons with the frequency close to one half of the pumping frequency, i.e., ν_p=4.05 GHz. These primary magnons actively interact with each other through the fast nonlinear four-wave magnon-magnon interaction. As a result a quasi-equilibrium distribution of secondary thermalized magnons over the spectrum is established after the thermalization time less than 100 ns, which is much smaller than the characteristic spin-lattice relaxation time ($\tau_{sl} > 1000$ ns).

In order directly to probe the distribution of magnons over frequencies the Brillouin light scattering (BLS) spectroscopy was used. A probing beam from an Ar^+-ion laser with the wavelength of $\lambda = 514$ nm and the power of 10 mW was focused onto the pumping resonator. The laser beam passed through the film, was diffusively reflected from the resonator, passed through the film again, was collected by an objective, and was sent to a multi-pass tandem Fabry-Perot interferometer for a frequency analysis. Usually, the BLS technique is characterized by selectivity with respect to the wavevectors of detected magnons. However, the use of a short-focus and wide-aperture objective together with the diffusive reflection of light by the pumping resonator provided an efficient way to detect magnons in a wide interval of the in-plane wavevectors up to the maximum wavevector of $K = 2 \cdot 10^5$ cm^{-1} as indicated in figure 1. This wavevector interval definitely covers the bottom of the magnon spectrum close to $k_{min} \approx 5.5 \cdot 10^4$ cm^{-1} where the BEC of magnons should occur. A typical frequency resolution of the experimental setup was $\Delta\nu = 250$ MHz. It was also possible to achieve a better resolution of $\Delta\nu = 50$ MHz, albeit at the expense of sensitivity. The analysis of scattered light was performed in a stroboscopic regime with the temporal resolution of 100 ns. Each spectrum corresponding to a given delay time t with respect to the start of the pumping pulse is obtained by accumulating over the time interval (t, t + 100 ns).

Figure 3 shows the measured BLS spectra reflecting the distributions of magnons over frequencies at different powers of the parametric pumping P. The spectra were recorded at the end of the pumping pulse, i.e., at $t = 900$ ns. As it will be shown below (see figure 4) a steady state of the driven magnon gas, corresponding to the flow equilibrium between the pumping and the spin-lattice relaxation, is formed at such long delay time. From the theoretical point of view the measured BLS intensity $I(\nu)$ is proportional to the reduced spectral density of magnons, $I(\nu) \sim \tilde{D}(\nu) n(\nu)$, where $\tilde{D}(\nu)$ is the density of magnon states taking into account

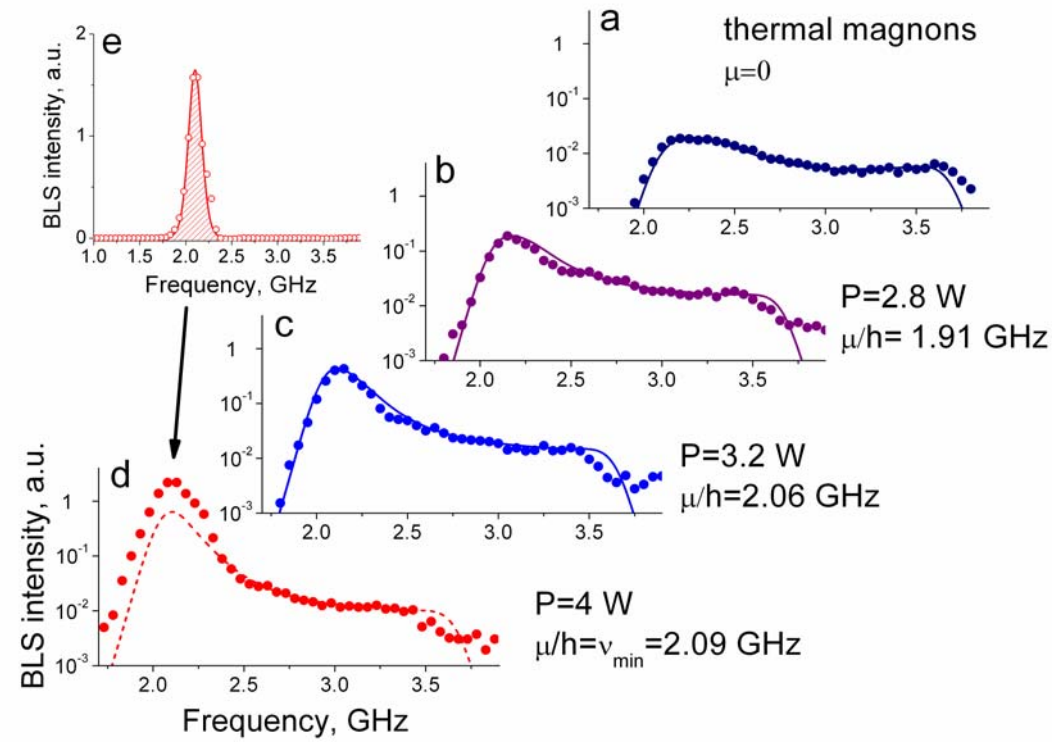

Figure 3. BLS spectra obtained for different pumping powers P. (a) – spectrum for thermally excited magnons, (b)-(d) – spectra for pumping powers P=2.8, 3.2, 4 W, respectively. The dots show the experimental data, the lines are the result of calculations as described in the text. (e) – difference between the experimental spectrum obtained for the pumping power $P = 4$ W and the spectrum calculated using $\mu = \mu_{max}$. The dots show the result of subtraction, the line represents the apparatus function of the setup with the finite frequency resolution of the interferometer taken into account.

only the magnons accessible for BLS (i.e., the magnons with in-plane wavevectors $|k| < K$) and $n(\nu)$ is the occupation function of magnon states. Since the value of the chemical potential at the thermal equilibrium with the lattice is known ($\mu = 0$), $\tilde{D}(\nu)$ can be determined from a BLS spectrum $I(\nu)$ recorded without pumping using $n(\nu, \mu = 0)$. This spectrum is shown in figure 3(a). The dots correspond to the experimental data, whereas the solid line represents the calculated $I(\nu)$ with $\tilde{D}(\nu)$ being a fit function. First, a probing function $\tilde{D}(\nu)$ was calculated using the approach developed in [28] taking into account the finite interval of wavevectors accessible for BLS. The parameters determining $\tilde{D}(\nu)$ (material parameters of the YIG film and the maximum wavevector K accessible for BLS) were then varied to achieve the best coincidence of calculated $I(\nu)$ with the experimental results. The function $\tilde{D}(\nu)$ obtained in such a way does not demonstrate any singularities. It shows a broad maximum at lower frequencies. In fact, this maximum is not an intrinsic feature of the

magnon spectrum. It originates from the limited sensitivity of the measurement technique with respect to magnons with large wavevectors corresponding to higher frequencies.

The obtained function $\tilde{D}(\nu)$ was used to analyze the magnon distributions obtained for the magnon gas driven by means of the parametric pumping. The corresponding BLS spectra for three different values of the pumping power P= 2.8, 3.2, 4 W are shown in figures 3(b)-3(d) by dots. As seen from the figures, the shapes of the BLS spectra are modified with increasing pumping power reflecting the growth of μ. At the same time the spectral density of magnons near the bottom of the spectrum grows significantly (note the logarithmic scale of the graphs). From the fit of the BLS spectra (solid lines in figures 3(a)-3(c)), based on the Bose-Einstein statistics, the values of μ for different pumping powers were obtained. These values are indicated close to the corresponding graphs. At the pumping power of 3.2 W the corresponding value of the chemical potential μ/h = 2.06 GHz is very close to its critical value $\mu_{max}/h = \varepsilon_{min}/h = \nu_{min}$ = 2.09 GHz. Furthermore, at the pumping power of 4 W the occupation numbers close to ν_{min} are so large that the measured spectrum cannot be described using the occupation function (1). To demonstrate this fact the calculated distribution $I(\nu)$ corresponding to the occupation function with the largest possible chemical potential $n_c(\nu, \mu = \mu_{max})$ is shown in figure 3(d) by dashed line. As seen from the figure, the difference between the measured spectrum and the spectrum calculated taking $n_c(\nu, \mu = \mu_{max})$ exists close to ν_{min} only. Figure 3(e) corroborating this conclusion represents the same difference in the linear scale. To explain the experimental results demonstrating an overpopulation of the magnon states close to ν_{min} one needs to postulate a formation of a condensate at the bottom of the magnon spectrum. The overpopulation of magnon states due to the formation of Bose-Einstein condensate should be proportional to $\delta(\nu-\nu_{min})$. However, due to a finite experimental frequency resolution the δ-peak appears in the experiment as a peak proportional to the apparatus function of the measurement setup, which is shown in figure 3 (e) by the solid line. As seen from the figure, the agreement between the experimental data and the apparatus function is convincing. Additional measurements with the best achieved frequency resolution of 50 MHz have confirmed that the spectral width of the observed peak at ν_{min} is below the experimental resolution.

Concluding this discussion let us emphasize that the observed narrowing of the magnon distribution in the energy space is tremendous. In fact, at the thermal equilibrium the magnon states from ν_{min} to $\nu_{th} \sim k_B T_0/h$ are occupied, whereas the width of the peak in figure 3(e) is below $10^{-5}\nu_{th}$. We consider this fact is a strong evidence that the magnon Bose-Einstein condensation is observed. Even stronger evidence would be a direct observation of the spontaneous spatial coherency of magnons accumulated at the minimum frequency ν_{min}. Such a direct observation could be realized if one would be able to investigate the created

condensate with an appropriate spatial resolution. This is the subject of further investigations. Let us emphasize that due to the relatively large wavevector of magnons at the bottom of the spectrum corresponding to the wavelength of about 1 μm this direct observation is not trivial. A recently developed micro-focus BLS setup characterized by a spatial resolution of down to 250 nm [29] will be applied for these studies.

In the above discussions we considered the steady state of the parametrically driven magnon gas at relatively large delays with respect to the start of the pumping pulse. As was already mentioned, the used experimental technique also allows one to measure magnon distributions corresponding to different stages of the pumping process with a temporal resolution. Applying the analysis similar to that used above (see figure 3) to BLS spectra measured at different delays with respect the start of the pumping pulse, the parameters of the magnon gas were monitored. As a result, the temporal evolution of the chemical potential was determined for different pumping powers. The results are presented in figure 4. As seen from the figure, the chemical potential of the magnon gas grows, as the total number of the magnons increases due to the continuous injection of additional particles by the pumping. For small powers (P = 2.8 W and 3.2 W) the chemical potential increases asymptotically approaching to a steady value, determined by the balance between the positive flow of magnons from the pumping and the negative flow of magnons due to the spin-lattice relaxation. However, at P = 4 W the growth of the chemical potential is completely different: at the delay time t = 300 ns the chemical potential reaches its maximum value $\mu_{max} = h\nu_{min}$. After that it remains constant up to

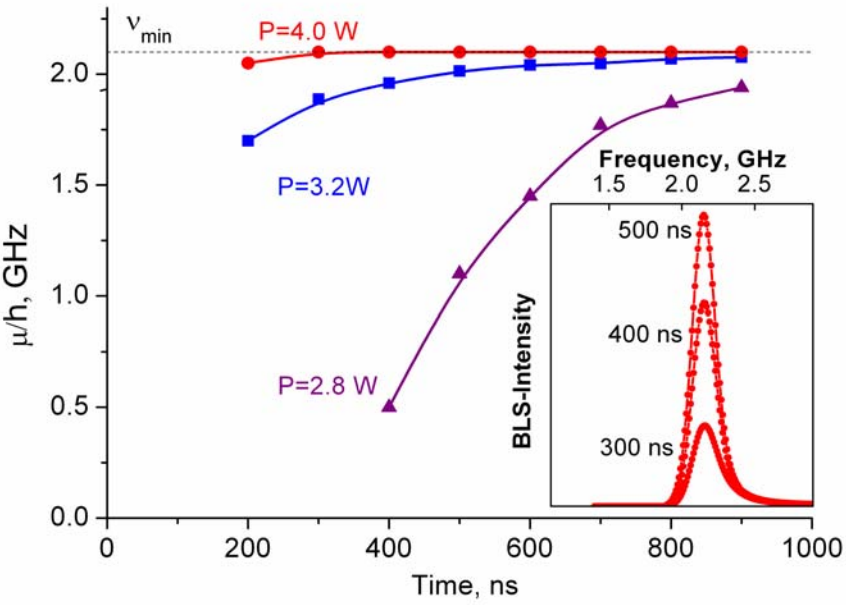

Figure 4. Temporal dependence of the chemical potential of magnon gas for different pumping powers P. Dots – experimental results, lines – guides for the eye. Inset: the low-frequency parts of the BLS spectra for P = 4 W recorded at different delay times.

the end of the pumping pulse. At the same time the magnon density close to the bottom of the magnon spectrum continues to grow, which results in the increasing amplitude of the condensate peak (see the inset in figure 4). Note that for pumping powers smaller than 3.2 W the chemical potential does not reach the minimum magnon energy at delays up to 900 ns and the condensate can not form.

The temporal resolution of the measurement technique also allows one to study the relaxation of the magnon gas after the pumping pulse is switched off. The magnon distributions measured at different delays after the pumping process is finished at t_p=1000 ns are shown in figure 5. A distribution corresponding to the end of the pumping pulse (t = 900 ns, i.e., integration interval 900-1000 ns) is shown for comparison as well. The figure clearly demonstrates a difference of the relaxation rates of the condensate and the rest part of magnons. In fact, the density of magnons far away from ν_{min} decreases by a factor of 10 during the first 200 ns after the end of the pumping pulse, while the density of the condensate shows almost no changes. This effect can be associated with kinetics of the magnon distribution over the spectrum. Even after the pumping is switched off magnons from the upper part of the spectrum continue to scatter into the condensate due to the four-wave magnon-magnon interaction processes and support its existence. The study of the condensate relaxation and its stability will be a subject of our further investigations.

The obtained results clearly show that magnetic systems represent a very promising medium for experimental investigations of Bose-Einstein condensation. In particular, they provide a unique possibility to achieve BEC transition at room temperature. Besides, the spectrum of magnons in ferromagnetic films demonstrates certain interesting features, which can lead to a

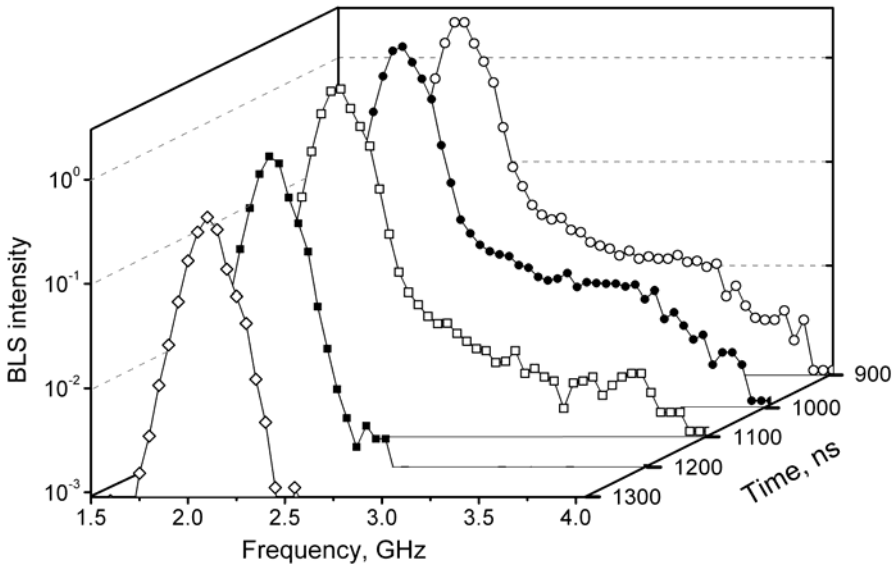

Figure 5. Evolution of the magnon distribution corresponding to P = 4 W after the pumping pulse is switched off. Dots – experimental results, lines – guides for the eye.

discovery of novel effects connected with Bose-Einstein condensates. One of them is that the state with the lowest energy of the magnon gas is double-degenerate. There are two points in the magnon phase space corresponding to the minimum energy $\nu_{\min}$: $k = \pm k_{\min}$.(see figure 1). The pumping procedure does not break this symmetry: two primary magnons with opposite wavevectors are created by each photon of microwave pumping. Thus, one can expect that the magnon accumulation starts simultaneously at two points of the phase space. Correspondingly, two condensates with $k = \pm k_{\min}$ symmetrically occupy both points. This should result in an appearance of a standing wave of the condensate density in the real space. We consider the use of this feature of the magnon condensate as a promising way directly to probe its coherency and determine the wavelength of magnons building the condensate. In general, we believe that the unique properties of magnetic systems will bring new ideas to the physics of Bose-Einstein condensation and stimulate further development of the area of magnonics and nonlinear high-frequency magnetization dynamics.

In conclusion, a quasi-equilibrium gas of magnons with a non-zero chemical potential is created using microwave parametric pumping. The value of the chemical potential in this gas of magnons is controlled by the pumping power. For a certain critical value of the pumping power the Bose-Einstein condensation of magnons occurs. The distinguishing feature of this condensation is that it takes place in a dense magnon gas in the dynamic (pumping-induced) quasi-equilibrium state at room temperature.

Support by the Deutsche Forschungsgemeinschaft, US Army Research Office, and by the Science & Technology Center of Ukraine is gratefully acknowledged.

References

[1] Einstein A 1925 Quantentheorie des einatomigen idealen Gases, *Sitzungsberg. Ber. Preuss. Akad. Wiss.* **1** 3-14

[2] Anderson M H, Ensher J R, Matthews M R, Wieman C E and Cornell E A 1995 *Science* **269** 198-201

[3] Davis K B, Mewes M -O, Andrews M R, van Druten N J, Durfee D S, Kurn D M and Ketterle W 1995 *Phys. Rev. Lett.* **75** 3969-73

[4] L´vov V S 1994 *Wave Turbulence Under Parametric Excitation* (Berlin, Heidelberg: Springer-Verlag)

[5] Hulin D, Mysyrowicz A and Benoit a la Guillaume C 1980 *Phys. Rev. Lett.* **45** 1970-3

[6] Snoke D 2006 *Nature* **443**, 403-4

[7] Snoke D W and Wolfe J P 1989 *Phys. Rev. B* **39** 4030-7

[8] Fukuzawa T, Mendez E E and Hong J M 1990 *Phys. Rev. Lett.* **64** 3066-9

[9] Butov L V 2004 *J. Phys.: Condens. Matter* **16** R1577-613

[10] Eisenstein J P and MacDonald A M 2004 *Nature* **432** 691-4

[11] Yamamoto Y 2000 *Nature* **405** 629-30

[12] Kasprzak J *et al.* 2006 *Nature* **443**, 409-14

[13] Misochko O V, Hase M, Ishioka K and Kitajima M 2004 *Phys. Lett. A* **321** 381-7

[14] Nikuni T, Oshikawa M, Oosawa A and Tanaka H 2000 *Phys. Rev. Lett.* **84** 5868-71

[15] Rüegg N, Cavadini A, Furrer H -U Güdel K, Krämer H, Mutka A, Wildes K, Habicht and Vorderwisch P 2003 *Nature* **423** 62-5

[16] Coldea R, Tennant D A, Habicht K, Smeibidl P, Wolters C and Tylczynski Z 2000 *Phys. Rev. Lett.* **88** 137203

[17] Radu T, Wilhelm H, Yushankhai V, Kovrizhin D, Coldea R, Tylczynski L, Lühmann T and Steglich F 2005 *Phys. Rev. Lett.* **95** 127202

[18] Jaime M *at al*. 2004 *Phys. Rev. Lett.* **93** 087203

[19] Demokritov S O, Demidov V E, Dzyapko O, Melkov G A, Serga A A, Hillebrands B and Slavin A N 2006 *Nature* **443**, 430-3

[20] Lax B and Button K J 1962 *Microwave Ferrites and Ferrimagnets* (New York: McGraw-Hill Book Company Inc.)

[21] Gurevich A G and Melkov G A 1996 *Magnetization Oscillations and Waves* (New York: CRC Press)

[22] Demokritov S O, Hillebrands B and Slavin A N 2001 *Phys. Rep.* **348**, 441-89

[23] Damon R W and Eshbach J R 1961 *J. Phys. Chem. Sol.* **19** 308-20

[24] Kalinikos B A and Slavin A N 1986 *J. Phys. C* **19** 7013-33

[25] Landau L D and Lifshitz E M 1980 *Statistical Physics* (Oxford: Butterworth-Heinemann)

[26] Melkov G A and Sholom S V 1991 *Zh. Eksp. Teor. Fiz.* **99** 610-8; translation: 1991 *Sov. Phys. JETP* **72** 341-6

[27] Demidov V E, Dzyapko O, Demokritov S O, Melkov G A and Slavin A N ”Thermalization of a parametrically driven magnon gas leading to Bose-Einstein condensation”, submitted to Physical Review Letters.

[28] Sparks M 1970 *Phys. Rev. B* **1** 3831-56

[29] Demidov V E, Demokritov S O, Hillebrands B, Laufenberg M and Freitas P P 2004 *Appl. Phys. Lett.* **85**, 2866-8